Holmberg H, Ahtila P. Comparison of drying costs in biofuel drying between multi-stage and single-stage drying. Biomass & Bioenergy 2004; 26: 515-530.

Available online at www.sciencedirect.com
SCIENCE DIRECT®
Biomass and Bioenergy 26 (2004) 515–530
BIOMASS & BIOENERGY
www.elsevier.com/locate/biombioe

Comparison of drying costs in biofuel drying between multi-stage and single-stage drying

Henrik Holmberg*, Pekka Ahtila

Helsinki University of Technology, P.O.Box 4400, FIN-02015 Hut, Finland

Received 16 January 2003; received in revised form 4 September 2003; accepted 26 September 2003

Abstract

The moisture content of wood-based biofuels (bark, forest residues, and waste wood) used by the forest industry typically varies between 50 and 63 w-%. The high moisture content considerably decreases the power production of the power plant. The main target of this paper is to compare the drying costs of two alternative drying systems: multi-stage drying, and single-stage drying with multi-stage heating. Air is used as a drying gas in both systems and is heated in indirect heat exchangers. Secondary heat, back pressure steam, and extraction steam are available for heating the drying air. Both capital and running costs are included in the drying costs. The drying systems are compared in example cases where the availability of heat sources, amortisation time, and price of elecricity are different. According to results, single-stage drying is usually a more economic drying system when the amortisation time is short. However, the competitiveness of multi-stage drying improves as the amortisation time becomes longer.

Keywords: Multi-stage drying; Single-stage drying; Biofuel; Drying costs

1. Introduction

In Finland, bark, forest residues, and different kinds of waste wood represent approximately 19 % of the total primary fuel consumed by the forest industry [1,2]. The term waste wood refers to by-products of the mechanical forest industry (e.g. sawdust, chips) that can be utilised in energy production. Biofuels are usually burnt in fluidised-bed boilers to produce heat and electricity for the mill. The power generation process is based on the well-known Clausius–Rankine steam process. The moisture content of these bio fuels typically varies between 50 and 63 w-% (water per total mass) depending on the season, weather and type of bio fuel. The typical lower heating value (net caloric heating value) of dry bio fuels varies from 18.5 to 21 kJ/kg [3]. The energy needed for the evaporation of water in the combustion chamber cannot be utilised in the power generation process (the temperature level of the heat recovery is too low), and therefore high fuel moisture decreases the energy input into this process. Because electricity production is proportional to energy input, it decreases as a result of fuel moisture. If the fuel moisture is, say, 60 w-%, and the heating value of the dry fuel, say, 20 kJ/kg, the energy input into the steam process is 18% lower than that in the case of the dry fuel. Additionally, the variation of the fuel moisture makes the operation of the boiler more difficult.

* Corresponding author.
E-mail address: henrik.holmberg@hut.fi (H. Holmberg).

0961-9534/$ - see front matter © 2003 Elsevier Ltd. All rights reserved.
doi:10.1016/j.biombioe.2003.09.007

Nomenclature

A	Area (m^2)
B	Breadth (m)
b_e	Price of elecricity (€/MWh)
b_h	Price of heat (€/MWh)
C	Costs (€)
c	Specific heat capacity (kJ/kgK)
L	Length (m)
$\dot{m}$	Air mass flow (kg_{da}/s)
$\dot{M}$	Fuel mass flow (kg_{dm})
p	Pressure (Pa)
t	Temperature (°C)
u	Fuel moisture (kg/kg_{dm})
v	Velocity (m/s)
x	Air moisture (kg/kg_{da})
Z	Height (m)

Greeks

ε	Volume fraction of air (-)
η	Efficiency (-)
Φ	Heat effect (W)
ρ	Density (kg/m^3)
τ	Time (s)

Subscripts

a	air
c	conveyor
da	dry air
dm	dry mas
f	fuel
p	particle

Biofuels are not dried in paper and pulp mills in Finland at the moment. Although high moisture content decreases power production, it is possible to combust a biofuel which has a moisture content of approximately 62–65% in fluidised boilers [4]. At higher moisture contents, support fuel is needed to keep the combustion stable. All wood-based fuel contain volatile organic compounds (VOC) that may be emitted during drying. In many countries, there are legal restrictions on the amounts that may be released [5]. The potential emissions must be taken into account, which sets further requirements for the design of the dryer.

Interest in biofuel drying has, however, increased in the forest industry recently. This paper focuses on biofuel drying in a pulp and paper mill when three different heat sources—secondary heat, back pressure steam, and extraction steam are available for drying energy. Air is used as a drying medium and heat transfer into the drying system occurs in indirect heat exchanges.

The main target is to evaluate how the drying process should be carried out in order to minimise drying costs. Two alternative drying systems, multi-stage drying, and single-stage drying with multi-stage heating, are compared in example cases where the most essential boundary conditions of the drying process are different. Both capital and running costs are included in the drying costs. A continuous crossflow dryer where air passes through the perforated tray and the bed is used as the dryer construction in both systems.

2. Description of drying systems

The energy sources with the greatest potential for biofuel drying in a pulp and paper mill are secondary heat, back pressure steam, and extraction steam. In this connection, secondary heat (also known as waste heat) means heat recovered to a heat recovery system from energy flows leaving the main processes. The circulation fluid in the heat recovery system is usually water, and the temperatures of the available secondary heat flows are typically in the range of 50–90°C. The pressure of back pressure steam is typically 3–4 bar (ca. 133–144°C) and the pressure of extraction steam 10–12 bar (ca. 179–187°C). The drying temperature is usually 5–10°C lower than the temperature of the heat source, depending on the minimum temperature difference between the heat source and the drying air in the heat exchanger. Fig. 1 illustrates the mass and energy balances of the adiabatic drying process utilising these three heat sources.

Because the drying temperatures are relatively low when secondary heat is used (around 60–80°C) the dimensions of the dryer become larger than if higher drying temperatures are used. Back pressure and

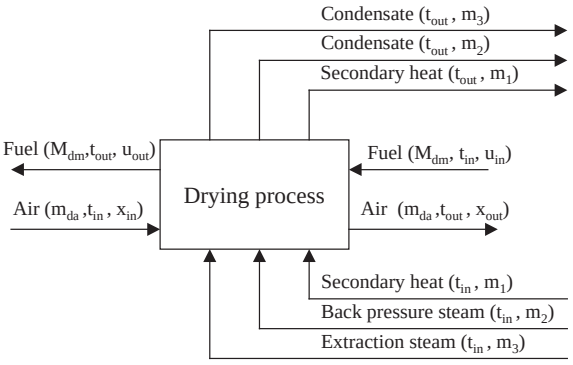

Fig. 1. Mass and energy balance of adiabatic drying.

extraction steam represent, however, more valuable energy than secondary heat, because by letting the steam expand in a turbine it is possible to get mechanical work (electricity) out of the steam process. In pulp and paper mills, the cost of secondary heat is usually close to zero and cost of steam depends on the pressure. So, one can state that in comparison to the use of steam secondary heat increases capital costs but decreases operating costs. In addition, the availability of heat sources for drying energy is limited. Low-temperature secondary heat is usually widely available but the availability of higher temperature heat sources (steam and hot waters) is more limited.

Two alternative ways to construct the drying process (see Fig. 2) are considered in this paper: multi-stage drying and single-stage drying with multi-stage heating. Both drying systems are shown in Fig. 2. A drying stage consists of a heating period and a drying period. Fig. 3 illustrates how the air moisture changes in the Mollier diagram in these two systems.

The evaporation rate is the product of the air mass flow and the change of air moisture. Fig. 3 shows that the change of air moisture is greater in multi- than in single-stage drying. This means that the air mass flow is smaller in multi-stage drying. It is, however, possible that the dimensions of the multi-stage dryer are bigger, because the drying air must pass through several drying stages. Dryer dimensions are proportional to product $n\dot{m}_{da}$, where n is the number of drying stages.

To reach the highest possible temperature in single-stage drying, there must be enough steam to heat the air mass flow needed for drying. The air demand in drying depends on many drying parameters, and also the type of dryer. The determination of air mass flow in continuous crossflow drying is focused on in this paper. If there is not enough steam available, the highest air temperature remains clearly lower than the temperature of the extraction or back pressure steam.

The emissions released during drying are heavily dependent on the drying temperature [6]. Usually, the amounts of emissions increase considerably when the drying temperature is above 100°C (see Fig. 4). Because of the emissions, the exhaust air from the dryer cannot be released into the atmosphere, if the drying temperature is over 100°C. To eliminate the release of emissions during drying, the exhaust air from the dryer is added to combustion air. If the drying temperature is below 100°C, it is usually possible to discharge the exhaust air into the atmosphere. Fig. 2 shows that part of the exhaust air from the first drying stage can be discharged into the atmosphere in multi-stage drying.

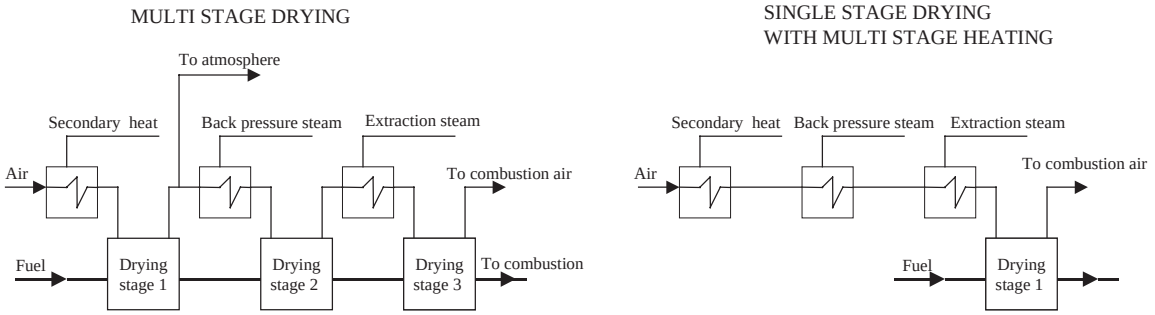

Fig. 2. Multi-stage drying and single-stage drying with multi-stage heating.

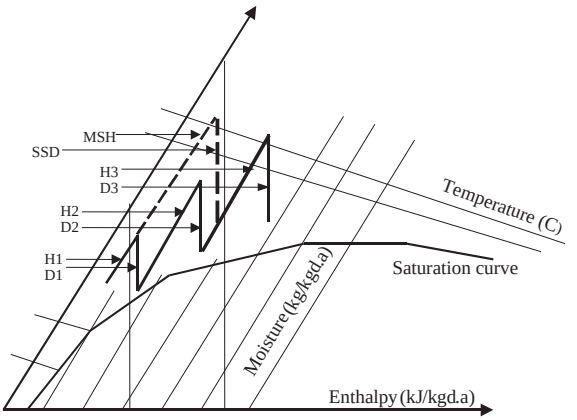

Fig. 3. Change of air moisture in the Mollier diagram in multi- and single-stage drying. H =heating period in multi-stage drying and D=drying period in multi-stage drying. The broken line describes the drying process in single-stage drying (SSD) with multi-stage heating (MSH). The Mollier diagram is depicted as a Salin–Soininen perspective transformation [13].

This is possible because the air is heated by secondary heat, the temperature of which is clearly below 100°C. Because of the partial discharge of exhaust air, the air mass flow in the first drying stage may be greater than in other drying stages.

3. Drying costs

The classification of drying costs is mainly based on the principles presented in Ref. [7]. The drying costs consist of both capital and running costs. Capital costs are usually divided into direct and indirect costs. The drying costs $Cost_{\mathrm{D}}$ may be written as follows

$$Cost_{\mathrm{D}} = Cost_{\mathrm{DC}} + Cost_{\mathrm{IDC}} + Cost_{\mathrm{RUN}}, \quad (1)$$

where $Cost_{\mathrm{DC}}$ represents direct capital costs, $Cost_{\mathrm{IDC}}$ indirect capital costs, and $Cost_{\mathrm{RUN}}$ running costs.

Direct capital costs are calculated by multiplying purchased equipment costs by a given factor (the term "Lang factor" is used in [7]). Purchased equipment costs are frequently presented in chart form, and they are usually correlated with a capacity factor using the relationship

$$Cost_{\mathrm{eq}} = kY^{b}, \quad (2)$$

where k is the proportionality factor, Y the capacity parameter and b the exponent. Exponent b is typically within a range of 0.4–0.8 [7]. In drying systems, the main pieces of equipment are conveyors, heat exchangers, and fans. Regardless of the original capacity factor of each piece of equipment (e.g. cross-sectional area in the case of conveyors), they are all dependent

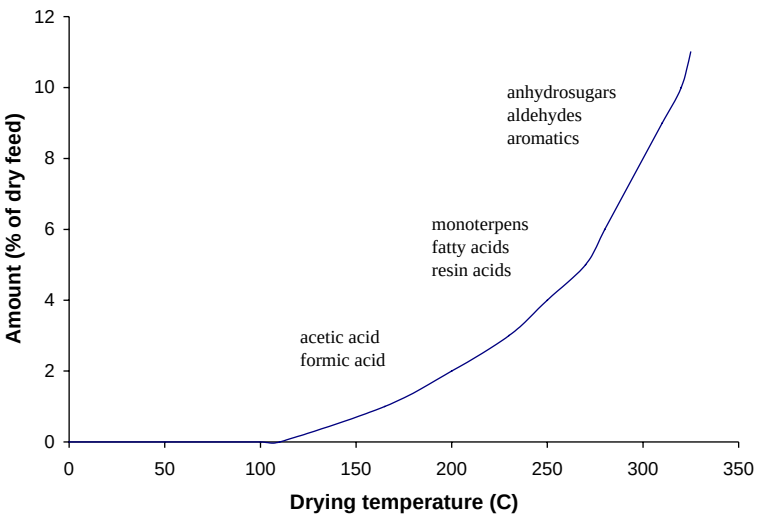

Fig. 4. Total amount and nature of organic compounds released in the atmospheric drying of biomass at different temperatures [6].

on the dry mass flow of drying air. Therefore, the capacity factor for each piece of equipment in (2) is air mass flow. The cross-sectional area of the air ducts and the covering of the dryer are also proportional to the air mass flow. If the length of the air ducts and the height of the dryer are estimated, their costs can be expressed as a function of air mass flow, too. Cost data for dryer equipment are obtained from published data sources, equipment seller quotations, and constructors. Proportionality factor a and exponent b in (2) are determined on the basis of the cost data.

The Lang factor is a sum of several factors which are applied for the estimation of costs, such as instrumentation, electrical, erection, structures, and lagging. The value of individual factor depends on the purchased equipment costs. Some approximative values for these factors are listed in [7]. Substituting air mass flow as the capacity parameter in (2) the direct capital costs of the dryer may be written as follows:

$$Cost_{\mathrm{DC}} = G\sum_{i=1}^{n} a_i \dot{m}_{\mathrm{da}}^{b_i}, \quad G = 1 + \sum_{j=1}^{m} g_j, \tag{3}$$

where n is the number of the pieces of equipment purchased, g the individual factor, and m the number of the factors. G represents the Lang factor in (3).

Indirect costs cover engineering and project management, as well as a contingency allowance, which can be considerable in pilot plans. Indirect costs are usually added as a percentage of direct capital costs, and they are not dependent on the dimensions of the dryer.

In drying, running costs encompass all those costs associated with the operation of the dryer. The most important running costs are composed of the use of heat and electricity and maintenance costs. The costs covering the use of heat and electricity are dependent on the annual operation time of the dryer and the price of energy. Maintenance costs are usually estimated as a percentage of direct capital costs, and typical values range from 2 % to 11%, averaging around 5% to 6% [7]. Personnel costs and insurance are also included in the running costs. They are, however, heavily site dependent and therefore more difficult to define. If the operating time of the dryer is τ h/year the annual running costs become

$$Cost_{\mathrm{RUN}} = \Phi\tau b_{\mathrm{h}} + P\tau b_{\mathrm{e}} + Cost_{\mathrm{m}} + Cost_x, \tag{4}$$

where Φ is the heat consumption (W), P the electricity consumption (W), b_{h} the price of the heat, b_{e} the price of the electricity, and $Cost_{\mathrm{m}}$ maintenance costs. The price of the heat depends on the heat source. The term $Cost_x$ represents all other running costs (e.g. personnel, and insurance).

Heat is used for the heating of drying air, and heat consumption may be calculated as follows:

$$\Phi = (c_{p\mathrm{da}} + x c_{pv})(t_2 - t_1)\dot{m}_{\mathrm{da}} \tag{5}$$

where $t_2 - t_1$ is the rise in air temperature in the heating. The main consumer of electricity is fans, and the consumption can be calculated as follows:

$$P = \frac{\Delta p}{\eta \rho_{\mathrm{da}}}\dot{m}_{\mathrm{da}}, \tag{6}$$

where Δp is the pressure drop of the dryer, η the mechanical efficient of the fan, and ρ_{da} the density of dry air.

4. Determination of drying air mass flow

To calculate the capital and running costs, the drying air mass flow for a given moisture decrease of the fuel must be defined. In this context, fuel moisture refers to average fuel moisture. Air mass flow is determined for a continuous crossflow dryer illustrated in Fig. 5. The derivation of air mass flow is based on the principles presented in [8,9]. The following initial assumptions are made:

- the dry mass flow of the fuel through the dryer is constant;
- the air velocity is constant;
- the bed height does not change during drying;
- the inlet air temperature and moisture are constant.

With the initial assumptions, the air mass flow $\dot{m}_{\mathrm{a}}$ and the dry mass flow of the fuel $\dot{M}_{\mathrm{f}}$ become

$$\dot{m}_{\mathrm{a}} = v_{\mathrm{a}} B L \rho_{\mathrm{da}}, \tag{7}$$

$$\dot{M}_{\mathrm{f}} = v_{\mathrm{c}} B Z (1 - \varepsilon)\rho_{\mathrm{dm}}, \tag{8}$$

where B is the breadth of the conveyor, v_{a} the air velocity, v_{c} the conveyor velocity, L length of the conveyor, and ε the volume fraction of air in the bed.

The value of the outlet air moisture changes depending on its position in the conveyor. Fig. 5 illustrates how the outlet moisture changes in a continuous

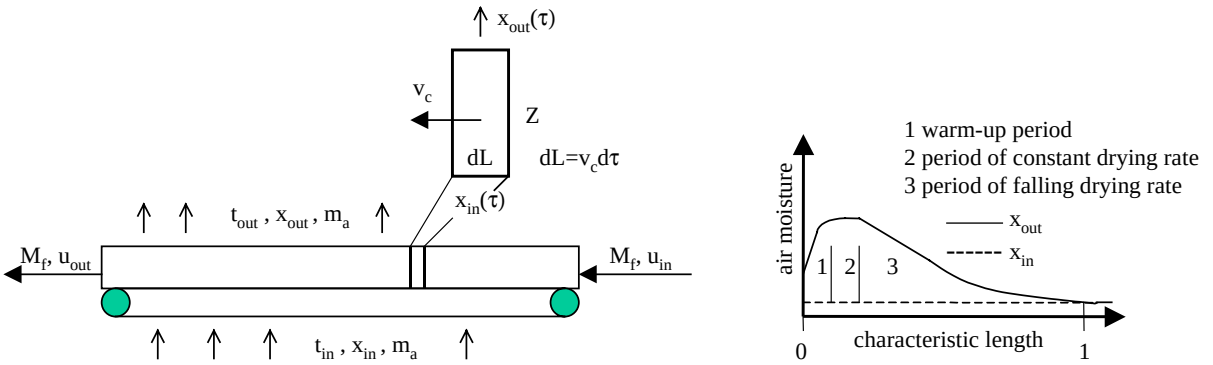

Fig. 5. A continuous crossflow dryer and the change of outlet air moisture during drying [8].

crossflow dryer [8]. Fig. 5 also shows the drying periods. The duration of the constant drying rate period depends on the material to be dried [9]. For example, according to [10] the duration of the constant drying rate is relatively short for wood-based material. As a result of a period of falling drying rate, the outlet air moisture constantly decreases.

If the time when the fuel enters the dryer is zero, the outlet moisture can be expressed as a function of drying time. If the bed height is given, the moisture balance between the air and the bed becomes

$$-v_c Z B(1-\varepsilon)\rho_{dm}\frac{\partial u}{\partial L}\,dL = v_a \rho_{da} B \sigma\, dL,$$

$$\sigma = x_{out}(\tau) - x_{in}(\tau), \tag{9}$$

where $x_{out}(\tau)$ is the air moisture after the bed as a function of drying time and $x_{in}(\tau)$ the air moisture before the bed which is usually constant. Substituting $dL = v_c\, d\tau$ in (9), the moisture balance becomes

$$\frac{du}{d\tau} = \frac{v_a \rho_{da}\sigma}{Z(1-\varepsilon)\rho_{dm}}. \tag{10}$$

The integration of (10) gives

$$u = u_{in} - \frac{v_a \rho_a}{Z\rho_{dm}}\int_0^\tau \sigma\, d\tau, \qquad u(0) = u_{in}. \tag{11}$$

The function σ is a complex function which depends on the following parameters:

$$\sigma(\tau) = f(t_a, t_p, x_{in}, v_a, Z, D_p, u, g(y_i)), \tag{12}$$

where t_p is the particle temperature, and D_p particle size. The function $g(y_i)$ represents the material parameters affecting the drying rate. These parameters are, for example density, heat conductivity, specific heat capacity, and permeability. It is usually hard to give any exact theoretical function for $\sigma(\tau)$. If it is possible to take readings of the outlet air moisture (for example, by measuring it), (11) may be rewritten as

$$u = u_{in} - \frac{v_a \rho_a}{Z\rho_{dm}}\sum_{i=1}^{n}\sigma_i \Delta\tau_i, \qquad \tau_u = \sum_{i=1}^{n}\Delta\tau_i, \tag{13}$$

where n is the number of intervals, $\Delta\tau$ the length of each interval, and τ_u the total drying time. If the drying time required to reach a desired outlet fuel moisture is τ_u, and (7) and (8) are combined, considering $L = v_c\tau_u$, the air mass flow becomes

$$\dot{m}_a = \frac{v_a \rho_a \dot{M}_{dm}}{Z(1-\varepsilon)\rho_{dm}}\tau_u. \tag{14}$$

The cross-sectional area of the dryer is obtained by dividing (14) by air density and air velocity.

Eqs. (13) and (14) give the air mass flow for a given fuel moisture decrease in a continuous crossflow drying. Although there are several parameters affecting the drying time and the air mass flow (see (12)), the only parameters that must be determined in (13) and (14) are bed height and, air velocity. Other parameters depend on the temperatures of the heat sources, the outdoor moisture and the material to be dried.

5. Bed height and air velocity

5.1. Bed height

The air mass flow is inversely proportional to the bed height (see (14)). Drying time is, however, dependent on the bed height; the higher the bed, the longer the drying time. An interesting question is how the ratio $\tau_u(Z)/Z$ behaves when the bed height is changed. In particular, it is interesting to see how the ratio behaves when the bed is so high that the air reaches its saturation point before the end of the bed. The value of the ratio also depends on the final moisture of the fuel.

The behaviour of the ratio $\tau_u(Z)/Z$ was experimentally studied. Regularly shaped wood particles were dried in a fixed-bed reactor; the bed height was changed and the other drying parameters were kept constant. The drying time was determined by measuring the values of the inlet and outlet air moistures as a function of time. The flow sheet of the reactor is shown in Fig. 6.

All the particles were ideal Norway spruce (Picea abies) particles of the same size and dimensions (length 20 mm, width 20 mm, thickness 5 mm). Two different air temperatures, 70°C and 120°C, were used. The inlet air moisture was 3 ± 0.5 g/kg$_{da}$ in each measurement. Air velocity per free sectional area of the grate before the bed was 0.6 m/s. The bed heights were changed by increasing and decreasing the number of the particles in a bed. Forty particles corresponded to a bed height of 2.5 mm. The length of the time interval was 5 s.

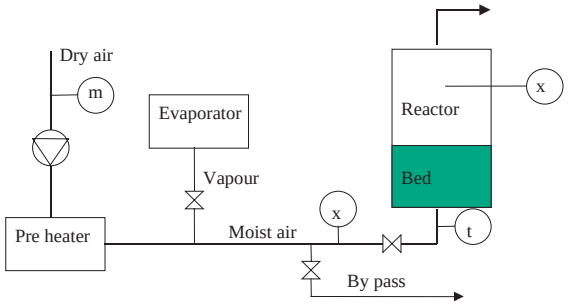

Fig. 6. Test rig with measurement points: x, air moisture; t, temperature; m, mass flow control.

Fig. 7 shows how the ratio $\tau_u(Z)/Z$ behaves as a function of bed height for various final moistures of the samples. The initial moisture of the sample in each test is 1.7 kg$_w$/kg$_{dm}$. The final moistures were calculated using Eq. (13).

Despite the final moisture of the sample, the ratio τ/Z seems to decrease constantly when the bed height increases. However, the derivative of the ratio is clearly smaller when the bed heights are over 80–100 and 100–120 mm for inlet temperatures of 70°C and 120°C, respectively. Fig. 8 shows that for an inlet temperature of 70°C the maximum moisture difference between outlet and inlet moisture does not change when the bed height is over 80 mm. This means that the outlet air is fully saturated during the first minutes of the drying. On the basis of these measurements, the bed must be at least so high that the drying air reaches its saturation point at the beginning of the drying. Because the pressure drop is proportional to the bed height, it is not reasonable to use a very high bed.

5.2. Air velocity

The cross-sectional area of the dryer is inversely proportional to air velocity, which means that the dryer dimensions and the investment costs decrease as a result of increased air velocity. In (14), the increased air velocity affects the drying time and the bed height. The drying time decreases as a result of improved mass transfer coefficient. The bed height can be raised because the air mass flow through the constant cross-sectional area increases and the air can absorb more water from the bed. This means that there must be more evaporation surface in the direction of the bed height, so that the air reaches its saturation point. On the other hand, the pressure drop is proportional to the square of the air velocity [11]. So, increased air velocity means higher running costs.

The theoretical upper limit for air velocity in fixed-bed drying is a minimum fluidising velocity. The minimum fluidising velocity depends on particle size, the density of the material, and the volume fraction of gas in the bed [11]. When the minimum fluidised-bed velocity is defined, it is important to consider that the density of material diminishes during the drying. If a drop in pressure does not impose any

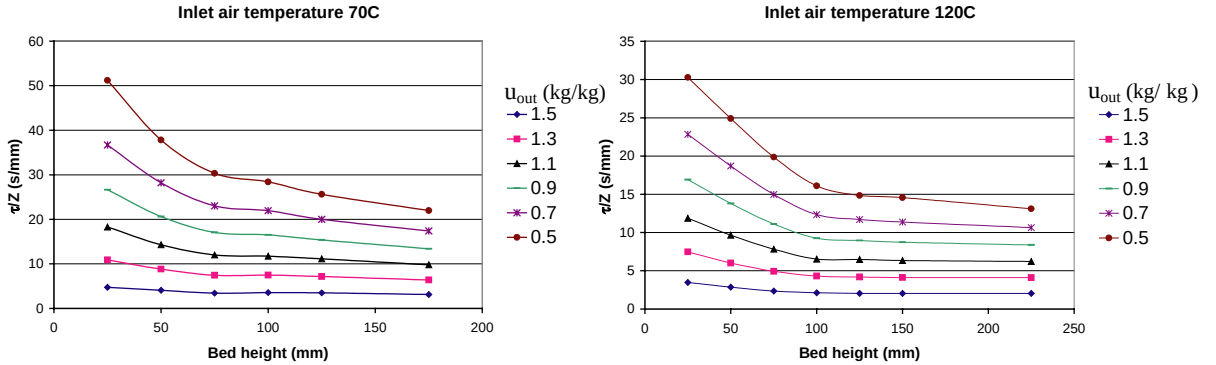

Fig. 7. The ratio τ/Z as a function of bed height for inlet temperatures 70°C and 120°C.

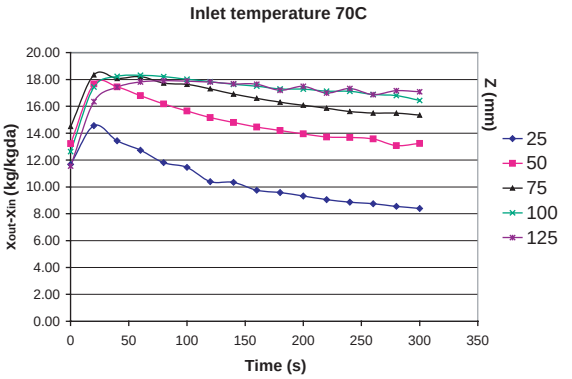

Fig. 8. Moisture difference $(x_{out} - x_{in})$ during the first 5 min of drying.

upper limits on air velocity, the optimal velocity is a little smaller than the minimum fluidising velocity.

6. Determination of cost functions for example drying systems

Cost functions are determined for multi- and single-stage drying by assuming there are three heat sources—secondary heat, back pressure steam, and extraction steam—available for drying.

6.1. Multi-stage drying

To minimise the drying costs in multi-stage drying, we should determine how much moisture from the fuel is removed in each drying stage when a constant dry mass flow of fuel moves through the dryer. It was mentioned before that all costs can be expressed as a function of air mass flow. In principle, (11) and (14) give the correlation between air mass flow and fuel moisture decrease. To calculate this correlation, (11) should be capable of being integrated. Unfortunately, it is usually impossible to integrate (11).

To avoid this problem, we assume that the fuel flow is divided into each drying stage according to Fig. 10. In this case, the fuel moisture decrease is constant in each drying stage, and we must determine what the dry mass flow of the fuel to each drying stage is. The air mass flow may be calculated using (13), and (14) for a given fuel moisture decrease. The change of air moisture $(x_{out}(\tau_i) - x_{in}(\tau_i))$ in (13) can be experimentally measured in a fixed-bed reactor. The results are analogous to continuous crossflow drying [12]. If it is assumed that the outlet air is perfectly mixed, the average values of the outlet air moisture and the temperature of the previous drying stage can be regarded as the new inlet values for the next drying stage.

Because there are three drying stages, the drying costs for each drying stage must be determined on the basis of the principles explained in the chapter "Drying costs". The cost function is the sum of these costs. The capital recovery factor is used to give the annual cost of recovering a investment. The value of the factor depends on the amortisation time and the interest. In the cost function (15), subscripts 1,2, and 3 refer to secondary heat, back pressure steam, and extraction steam, respectively. Fig. 9 shows other indices used in the cost function. The cost function with boundary

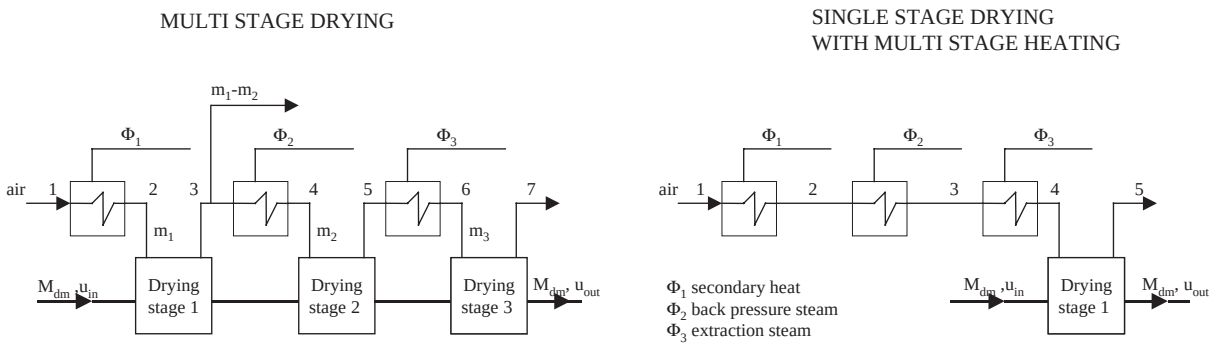

Fig. 9. Indices used in the cost functions.

conditions for multi-stage drying can be written as follows:

Cost function:

$$C(\dot{m}_1,\dot{m}_2,\dot{m}_3) = aG_1\sum_{i=1}^{n} k_i\dot{m}_1^{b_i} + aG_2\sum_{i=1}^{n} k_i\dot{m}_2^{b_i} + aG_3\sum_{i=1}^{n} k_i\dot{m}_3^{b_i} + \left(\dot{m}_1\frac{\Delta p_1}{\eta\rho_{da}} + \dot{m}_2\frac{\Delta p_2}{\eta\rho_{da}} + \dot{m}_3\frac{\Delta p_3}{\eta\rho_{da}}\right) b_e\tau + \dot{m}_1 c_{p1}(t_2-t_1)b_{h1}\tau + \dot{m}_2 c_{p2}(t_4-t_3)b_{h2}\tau + \dot{m}_3 c_{p3}(t_5-t_6)b_{h3}\tau + a\,Cost_{IDC} + Cost_m + Cost_x, \quad (15a)$$

where

$$\dot{m}_1 = y_1\frac{v_a\rho_a\dot{M}_{dm}}{Z_1(1-\varepsilon)\rho_{dm}}\tau_{u1},$$

$$\dot{m}_2 = y_2\frac{v_a\rho_a\dot{M}_{dm}}{Z_2(1-\varepsilon)\rho_{dm}}\tau_{u2},$$

$$\dot{m}_3 = y_3\frac{v_a\rho_a\dot{M}_{dm}}{Z_3(1-\varepsilon)\rho_{dm}}\tau_{u3}. \quad (15b)$$

Boundary conditions:

$$\Phi_1 \geqslant \dot{m}_1 c_{p1}(t_2-t_1), \quad (15c)$$

$$\Phi_2 \geqslant \dot{m}_2 c_{p2}(t_4-t_3), \quad (15d)$$

$$\Phi_3 \geqslant \dot{m}_3 c_{p3}(t_6-t_5), \quad (15e)$$

$$\dot{m}_1 \geqslant \dot{m}_2, \quad (15f)$$

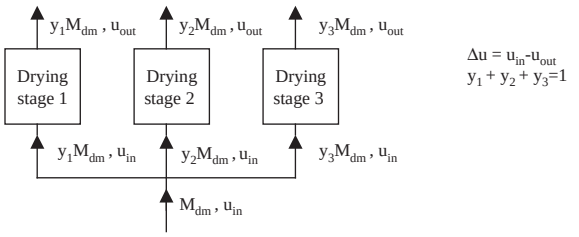

Fig. 10. Fuel input in multi-stage drying.

$$\dot{m}_2 = \dot{m}_3, \quad (15g)$$

$$y_1 + y_2 + y_3 = 1. \quad (15h)$$

In (15a), G is the Lang factor, n the number of the pieces of equipment, c_p the specific heat capacity ($c_p = c_{pda} + xc_{pv}$), τ the annual running time of the dryer, the capital recovery factor, $Cost_{IDC}$ the indirect capital costs, $Cost_m$ the maintenance costs, and $Cost_x$ the other costs associated with the operation of the dryer. The symbols k and b are constants associated with the definition of purchased equipment costs. In (15), y is the relative share of the fuel flow which is led to the drying stage, and τ_u is the drying time for a given fuel moisture decrease ($u_{in} - u_{out}$) in this drying stage (Fig. 10). The drying time τ_u is experimentally determined in a fixed-bed reactor for all drying conditions. If secondary heat is not used, (15f) is not valid. If back pressure or extraction steam is not used, (15g) is not valid.

Substituting (15b) in (15a) and (15c)–(15g), the cost function and the boundary conditions are expressed as a function of y_1, y_2, and y_3. The cost

function is a non-linear function, and boundary conditions are linear. In this case, it is usually possible to find values for y_1, y_2, and $y_3$minimising the cost function with given boundary conditions.

6.2. Single-stage drying

To determine the cost function for single-stage drying, there must be information about how the air demand in drying depends on the inlet air temperature. Next, we assume that there is a function which gives this dependence. In the cost function (16), subscripts 1,2, and 3 refer to secondary heat, back pressure steam, and extraction steam, respectively. Fig. 9 shows the other indices used in the cost function, and the capital recovery factor is again used to give the annual cost of recovering an investment. The cost function is expressed as a function of the air temperatures t_2 ,t_3, and t_4, and it may be written as follows:

Cost function:

$$C(t_2,t_3,t_4) = aG\sum_{i=1}^{n} k_i \dot{m}^{b_i} + \dot{m}\frac{\Delta p}{\eta\rho_{da}} b_e\tau + \dot{m}c_{p1}(t_2 - t_1)b_{h1}\tau + \dot{m}c_{p2}(t_3 - t_2)b_{h2}\tau + \dot{m}c_{p3}(t_4 - t_3)b_{h3}\tau + a\,Cost_{IDC} + Cost_m + Cost_x, \quad (16a)$$

where

$$\dot{m} = f(t), \quad t = t_4 - t_3 + t_3 - t_2 + t_2 - t_1 + t_1. \quad (16b)$$

Boundary conditions:

$$\dot{m}c_p(t_2 - t_1) \leqslant \Phi_1, \quad (16c)$$

$$\dot{m}c_p(t_3 - t_2) \leqslant \Phi_2, \quad (16d)$$

$$\dot{m}c_p(t_4 - t_3) \leqslant \Phi_3, \quad (16e)$$

$$t_1 \leqslant t_2 \leqslant t_{2max}, \quad (16f)$$

$$t_2 \leqslant t_3 \leqslant t_{3max}, \quad (16g)$$

$$t_3 \leqslant t_4 \leqslant t_{4max}. \quad (16h)$$

Boundary conditions (16c)–(16e) express how much each heat source can be used, at the maximum, in drying. Boundary conditions (16f)–(16h) take the second law of thermodynamics into account. According to the second law, heat cannot pass from a lower temperature to a higher one. This means that the maximum air temperature after the heat exchanger cannot be higher than the inlet temperature of the heat source. In practice, the maximum air temperatures t_{2max}, t_{3max}, and t_{4max} depend on the minimum temperature difference between air and heat source in a heat exchanger. The function $f(t)$ in (16b) can be experimentally determined in a fixed-bed reactor by measuring the drying time for various inlet air temperatures.

Substituting (16b) in (16a) and (16c)–(16h), the cost function and the boundary conditions are expressed as a function of t_2, t_3, and t_4. Both the cost function and the boundary conditions are non-linear. In this case, it may be more difficult to find a global minimum for the cost function.

7. Comparison example

The drying costs of these two drying concepts are compared in four example cases (A, B, C, D). It is assumed that there are always 8000 kW of secondary heat ($t = 78°C$), back pressure steam ($p = 4$ bar, $t = 138°C$), and extraction steam ($p = 10$ bar, $t = 180°C$) available for drying in each case. The amounts of heat available from each sources are, however, different in each case. The drying costs in cases A–C are compared by changing the amortisation time of the investment (interest 0%) and the final fuel moisture. The effect of the price of the electricity on the drying costs is considered in case D. The prices of steams are based on the price of the electricity that will be lost because the steam cannot expand to the lowest possible pressure in a turbine. The price of the secondary heat is mainly composed of the pumping costs. Therefore, the costs of the heat sources are dependent on the price of electricity. The initial values for each example case are shown in Table 1.

The material to be dried is regularly shaped spruce particles (length 20 mm, width 20 mm, thickness 5 mm). The initial moisture of the particles is 1.5 kg_w/kg_{dm}, and the dry mass flow of the material through the dryer is 1 kg_{dm}/s.

The temperature and moisture of the outdoor air are assumed to be 15°C and 0.0065 kg/kg_{da}. The

Table 1
Initial values in cases A–D

Case	Heat fluxes (MW)			Price of heat and electricity (Euro/MWh)				Amortisation time (year)	Final fuel moistures (kg/kg_{dm})
	Φ_1	Φ_2	Φ_3	b_{q1}	b_{q2}	b_{q3}	$b_{electricity}$		
A	4	2	2	0.2	3.6	6.0	25	1–35	0.2; 0.4; 0.6
B	6	1	1	0.2	3.6	6.0	25	1–35	0.2; 0.4; 0.6
C	2	3	3	0.2	3.6	6.0	25	1–35	0.2; 0.4; 0.6
D	4	2	2	0.12–0.56	2.2–10.3	3.6–16.9	15–70	1–35	0.2

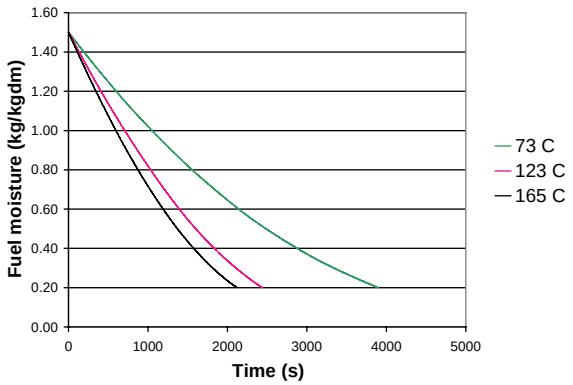

Fig. 11. Decrease of fuel moisture as a function of drying time for given inlet temperatures. Drying times are experimentally determined in a fixed-bed reactor, shown in Fig. 6.

maximum inlet air temperatures are 73°C, 123°C, and 165°C for secondary heat, back pressure steam, and extraction steam, respectively. The air mass flows at these temperatures are calculated using (13), and (14). The drying times for the inlet temperatures are experimentally determined in a fixed-bed reactor by measuring the outlet and inlet air moisture. The reactor is shown in Fig. 6. Fig. 11 shows the measured decreases of fuel moistures as a function of drying time. The bed heights are 100, 125, and 150 mm for the air temperatures 73°C, 123°C, and 165°C, respectively. The bed heights are chosen on the basis of the results shown in Fig. 7. The air velocity in each drying stage is 0.6 m/s.

In multi-stage drying, the inlet air moisture of the next drying stage is the outlet moisture of the previous drying stage. The inlet air moisture was only 0.003 kg/kg_{da} in each measurement, regardless of the air temperature. Because the inlet air moisture was lower than the moistures used in the example cases, the actual air temperatures in the measurements were also lower than 73°C, 123°C, and 165°C. The inlet moistures used in the example cases are listed in the appendix. The air temperatures in the measurements were determined in such a way that the temperature differences between dry bulb and wet bulb temperatures are the same as in the example cases. The actual inlet air temperatures were 70°C, 120°C, and 155°C. In single-stage drying, the air moisture is always 0.0065 kg/kg_{da}. However, we assume that the drying time in single-stage drying is the same as in multi-stage drying, despite the lower air moisture (this concerns only cases where inlet temperatures are higher than 73°C).

The purchased costs (in Euros) of the main equipment are calculated using the relationships which are shown in Table 2. The relationships for conveyors heat exchangers, and fans are determined on the basis of the cost information obtained from Finnish equipment seller quotations. The relationships for air ducts and covering are determined by assuming that they are black iron, the price of which is 3.5 €/kg and the density 9500 kg/m^3 (data obtained from a Finnish machine shop). The length and the wall thickness of the air ducts are assumed to be 30 m/drying stage and 3.5 mm, respectively. The air velocity inside the ducts is 10 m/s. The height and the wall thickness of the covering are assumed to be 8 and 3.5 mm, respectively. The cross-sectional area of the covering is 10% bigger than the cross-sectional area of the conveyor. All costs correspond to price levels for the year 2002. If the cost data have been obtained before this year (the years are listed in Table 2), a 5% annual increase in prices has been added to the original prices.

Table 2
Relationships for purchased equipment costs (in Euros)

Equipment	Relationship	Capacity parameter, Y	Additional parameter	Year
Conveyor	$2700Y$	Cross-sectional area of the conveyor		2000
Air–water heat exchanger	$9\Delta tY^{0,9}$	Air mass flow	Δt is temperature increase of air in heat exchanger	2000
Air–steam heat exchanger	$18\Delta tY^{0,9}$	Air mass flow	Δt is temperature increase of air in heat exchanger	2000
Air duct	$3770Y^{0,5}$	Air mass flow		2002
Fan	$0.9\Delta pY^{0,7}$	Air mass flow	Δp is pressure drop of drying stage	2002
Covering	$1200Y^{0,5}$	Cross-sectional area of the dryer		2002

The direct investment costs will be obtained by multiplying the purchased investment costs by a factor of 1.6. The factor takes into account costs such as instrumentation, lagging, etc., determined on the basis of the following values: electrical 0.1, instrumentation 0.1, lagging 0.05, civil work 0.15, installation 0.2. The quantities of the individual factors are roughly estimated on the basis of the values tabulated in [7]. It is, however, important to bear in mind that the actual value of the factor is heavily site dependent and can deviate considerably from that used. To estimate the factor more precisely, there should be detailed information about the investment costs concerning the dryer projects already carried out. Unfortunately, this information is not yet available. Indirect investment costs are usually not dependent on dryer dimensions, and they are assumed to be the same in each example case.

The operating costs associated with the use of heat and electricity are calculated on the basis of (5) and (6). The pressure drop is estimated to be 500 Pa for each drying stage in multi-stage drying. In single-stage drying, the pressure drop is assumed to be dependent on the number of heat exchangers, and is 500, 625, and 750 Pa for one, two, and three heat exchangers, respectively. Because the drying systems (single- and multi-stage drying) are always composed of similar main equipment, we assume that the maintenance costs and other costs associated with the operation of the dryer are the same for the both drying systems, given that they have the same initial values. By making this assumption the maintenance costs and other operating costs have no influence on the comparison of the drying systems, and it is not necessary to define these costs. The drying systems can be compared by calculating the difference between the drying costs (see Eq. (17)).

Table 3
Air demands for given final fuel moistures 0.2, 0.4, and 0.6 kg/kg_{dm}

Temperature (°C)	Air demand (kg/s)		
	0.2 kg/kg_{dm}	0.4 kg/kg_{dm}	0.6 kg/kg_{dm}
73	131	114	103
123	57	51	47
165	42	37	34

The air mass flows minimising drying costs in multi-stage drying are optimised using the Micro Soft Excel Solver. The air temperatures minimising drying costs in single-stage drying are assumed to be t_{2max}, t_{3max}, or t_{4max}. If there is enough heat available from each source, these temperatures represent temperatures where secondary heat is used first, then back pressure steam, and finally extraction steam. If there is not enough steam to heat the air flow to the temperatures t_{3max} or $t_{4max,}$ the drying costs are calculated at the highest possible temperatures which can be reached using first secondary heat and back pressure steam, and secondly secondary heat, back pressure steam, and extraction steam. It is, however, required that the air temperature be higher than 73°C in each case.

To find out the air mass flow in the temperature intervals 73–123°C, and 123–165°C, we assume that

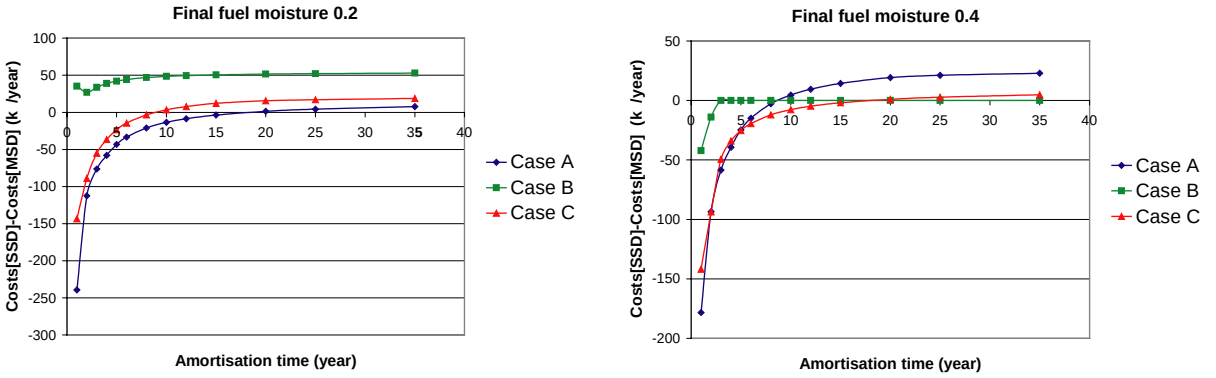

Fig. 12. Differences between drying costs for final fuel moistures 0.2 and 0.4 kg/kg_{dm}.

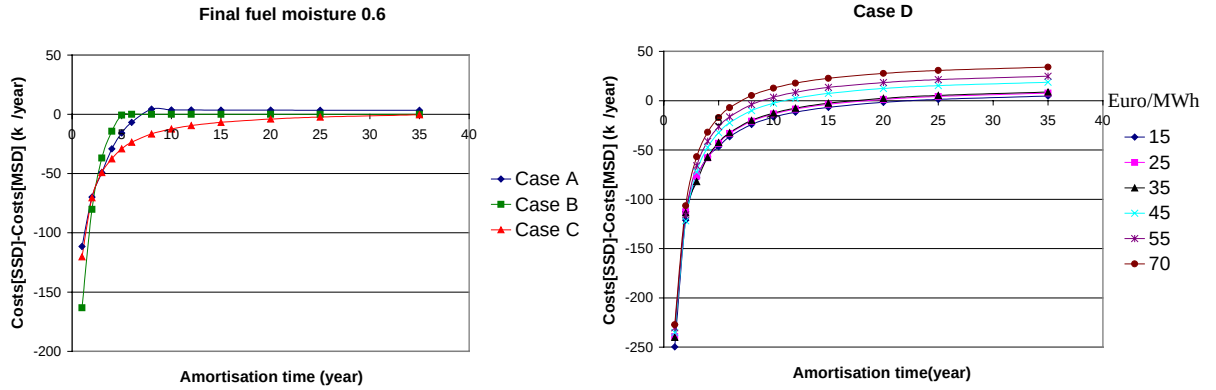

Fig. 13. Differences between drying costs for final fuel moisture 0.6 kg/kg_{dm}, and case D.

there is a linear connection between the inlet air temperature and drying air demand. The bed height is also assumed to be linearly dependent on the air temperature. The air demands for the given dry mass flow 1 kg_{dm}/s are the same as in multi-stage drying at the temperatures 73°C, 123°C, and 165°C. Table 3 shows the linear functions.

The drying costs for each calculation case are calculated using (15) and (16). The superiority of the drying systems is compared as a difference between the drying costs of single-stage drying (*SSD*) and multi-stage drying (*MSD*)

$$\text{Difference between drying costs} = Costs(SSD) - Costs(MSD). \quad (17)$$

If the difference between the drying costs is negative, single-stage drying is a more economic way to carry out the drying. If the difference is positive then multi-stage drying is a more economic drying system. Figs. 12 and 13 show the differences as a function of amortisation time between the drying costs for all example cases. A summary of the optimisation results and process values for both drying systems is shown in the appendix.

Figs. 12 and 13 show that the best drying system depends on the boundary conditions, and that the difference between the drying costs may also be remarkable. If the amortisation time is short, single-stage drying seems to be a more economic way to carry out the drying in most cases. This is a consequence of the lower annual capital costs of single-stage drying (see the appendix).

For a final fuel moisture of 0.2 kg/kg_{dm} multi-stage drying is, however, always a better system in case B. There is only 1 MW of back pressure steam and 1 MW

of extraction steam available for drying. Because of this, the highest air temperature which can be reached in single-stage drying is only 92°C, and the capital costs remain considerable.

For final fuel moistures 0.4, and 0.6 kg/kg_{dm} there is no difference between drying costs in case B, when the amortisation time is several years. It is the most economical way to carry out the drying using only secondary heat in both cases. In general, the use of secondary heat alone in drying may be a competitive alternative if the drying time is relatively short, even for a low drying temperature. For example, a reduction in particle size decreases the drying time considerably.

If the amortisation time is longer, multi-stage drying is generally a more economic drying concept. Because of the exhaust, the use of low-priced secondary heat can easily be maximised in multi-stage drying which decreases the running costs (see the appendix). For a final fuel moisture of 0.6 kg/kg_{dm}, single-stage drying is, however, a better drying concept in case C, because there is a small amount of secondary heat available.

The higher the price of electricity, the more economical as a drying concept the multi-stage drying is, because the use of secondary heat may be maximised in multi-stage drying.

8. Conclusions

Two alternative ways to carry out the biofuel drying in pulp and paper mill have been considered in the comparison examples by changing some of the most essential boundary conditions. If the amortisation time is short, single-stage drying is usually a more economic way to carry out the drying. If the amortisation time is long, more attention is paid to running costs and multi-stage drying is generally a more economic drying concept.

Although the cost functions are determined for a continuous crossflow dryer, the principle of the determination is the same for other kinds of dryer types, too. However, the calculation of the air mass flow depends significantly on the dryer type. It is, nevertheless, probable that the differences between drying costs in Figs. 12 and 13 behave basically in the same way for other dryer types, too.

Acknowledgements

This study has been financed by the Technology Centre of Finland (TeKes), Pohjolan Voima, Stora Enso, and Vapo. The authors gratefully acknowledge all those who contributed to this work.

Appendix

See Table 4 for a summary of the optimisation results and process values for multi- and single-state during systems.

Table 4
Summary of optimisation results

Case A: $\Phi_1 = 4000\ kW,\ \Phi_2 = 2000\ kW,\ \Phi_3 = 2000\ kW$
Multi-stage drying

Final fuel mositure (kg/kg_{dm})	Amortisation time (year)	m_1 (kg/s)	m_2 (kg/s)	m_3 (kg/s)	x_1, x_2 (kg/kg_{da})	x_3, x_4 (kg/kg_{da})	x_5, x_6 (kg/kg_{da})	x_7 (kg/kg_{da})	Investment costs (keuro)	Running costs (keuro)
0.2	1–3	30	19	19	0.0065	0.016	0.039	0.070	728	152
0.2	4–35	68	12	12	0.0065	0.016	0.039	0.070	884	106
0.4	1–2	15	15	15	0.0065	0.018	0.043	0.078	535	131
0.4	3	42	24	0	0.0065	0.018	0.043		658	73
0.4	4–35	68	13	0	0.0065	0.018	0.043		745	49
0.6	1	0	14	14		0.0065	0.034	0.071	359	129
0.6	2–3	23	23	0	0.0065	0.019	0.046		477	65
0.6	4–35	68	2	0		0.019	0.046		618	21

Table 4 (*Continued*)

Single-stage drying

Final fuel moisture (kg/kg_{dm})	Amortisation time (year)	m_1 (kg/s)	t_1 (°C)	t_2 (°C)	t_3 (°C)	t_4 (°C)	Investment costs (keuro)	Running costs (keuro)
0.2	1–2	42	15	73	120	165	475	166
0.2	3–35	58	15	73	107	125	587	122
0.4	1–2	31	15	73	125	165	365	122
0.4	3–21	43	15	73	118	125	452	83
0.6	21–35	64	15	73	104	104	598	76
0.6	1–2	24	15	73	125	165	283	92
0.6	3–7	33	15	73	125	125	350	59
0.6	7–35	72	15	69	73	73	622	24

Case B: $\Phi_1 = 6000\ kW,\ \Phi_2 = 1000\ kW,\ \Phi_3 = 1000\ kW$

Multi-stage drying

Final fuel mositure (kg/kg_{dm})	Amortisation time (year)	m_1 (kg/s)	m_2 (kg/s)	m_3 (kg/s)	x_1, x_2 (kg/kg_{da})	x_3, x_4 (kg/kg_{da})	x_5, x_6 (kg/kg_{da})	x_7 (kg/kg_{da})	Investment costs (keuro)	Running costs (keuro)
0.2	1–2	80	9	9	0.0065	0.016	0.039	0.07	932	91
0.2	3–35	101	13	0	0.0065	0.016	0.039		101	55
0.4	1–2	51	9	9	0.0065	0.018	0.043	0.078	680	84
0.4	3–35	97	0	0	0.0065	0.018			816	22
0.6	1–2	29	8	8	0.0065	0.019	0.046	0.084	492	78
0.6	3–35	72	0	0	0.0065	0.019			620	17

Single-stage drying

Final fuel moisture (kg/kg_{dm})	Amortisation time (year)	m_1 (kg/s)	t_1 (°C)	t_2 (°C)	t_3 (°C)	t_4 (°C)	Investment costs (keuro)	Running costs (keuro)
0.2	1–35	103	15	73	82	92	949	110
0.4	1–2	64	15	73	88	104	624	98
0.4	3–35	97	15	73	73	73	816	22
0.6	1	29	15	73	107	140	323	85
0.6	2–5	33	15	73	103	123	348	70
0.6	6–35	72	15	73	73	73	620	17

Case C: $\Phi_1 = 6000\ kW, \Phi_2 = 1000\ kW, \Phi_3 = 1000\ kW$

Multi-stage drying

Final fuel mositure (kg/kg_{dm})	Amortisation time (year)	m_1 (kg/s)	m_2 (kg/s)	m_3 (kg/s)	x_1, x_2 (kg/kg_{da})	x_3, x_4 (kg/kg_{da})	x_5, x_6 (kg/kg_{da})	x_7 (kg/kd_{da})	Investment costs (keuro)	Running costs (keuro)
0.2	1–2	0	24	24		0.0065	0.03	0.061	588	211
0.2	3	20	20	20	0.0065	0.016	0.039	0.07	687	163
0.2	4–35	34	18	18	0.0065	0.016	0.039	0.07	756	147
0.4	1–2	0	18	18		0.0065	0.032	0.067	457	165
0.4	3–35	34	28	0	0.0065	0.018	0.043		628	80
0.6	1	0	14	14		0.0065	0.034	0.072	359	129
0.6	2–3	23	23	0	0.0065	0.019	0.046		477	65
0.6	4–35	34	17	0	0.0065	0.019	0.046		518	54

Table 4 (*Continued*)

Single-stage drying

Final fuel moisture (kg/kg_{da})	Amortisation time (year)	m_1 (kg/s)	t_1 (°C)	t_2 (°C)	t_3 (°C)	t_4 (°C)	Investment costs (keuro)	Running costs (keuro)
0.2	1–6	42	15	62	125	165	479	177
0.2	17–35	58	15	49	125	125	600	170
0.4	1–3	31	15	73	125	165	361	120
0.4	4–35	43	15	60	125	125	453	90
0.6	1	24	15	73	125	165	275	92
0.6	2–35	33	15	73	125	125	350	57

Case D: $\Phi_1 = 4000\ kW$, $\Phi_2 = 2000\ kW$, $\Phi_3 = 2000\ kW$

Price of electricity	Multi-stage drying						Single-stage during			
(Euro/MWh)	Amort. time (year)	m_1 (kg/s)	m_2 (kg/s)	m_3 (kg/s)	Investment costs (keuro)	Running costs (keuro)	Amort. time (year)	m_1 (kg/s)	Investment costs (keuro)	Running costs (keuro)
15	1–5	30	19	19	728	91	1–4	42	475	98
15	6–35	68	12	12	884	64	5–35	58	587	73
25	1–3	30	19	19	728	152	1–2	42	475	166
25	4–35	68	12	12	884	106	3–35	58	587	122
35	1–2	30	19	19	728	212	1	42	475	230
35	3–35	68	12	12	884	149	2–35	58	587	171
45	1	30	19	19	728	274	1	42	475	295
45	2–35	68	12	12	884	192	2–35	58	587	219
55	1	30	19	19	728	334	1	42	475	361
55	2–35	68	12	12	884	235	2–35	58	587	268
70	1	30	19	19	728	426	1–35	58	587	341
70	2–35	68	12	12	884	299				

Subscripts refer to indices in Fig. 9.
Costs associated with the use of heat and electricity are only included in running costs.
Annual investment costs = (capital recovery factor) × (investment costs).

References

[1] www.pages of Finnish Forest Industry, http://english.forestindustries.fi/environment/energy/ 2001.

[2] www.pages of Finnish Statistics, http://www.stat.fi/tk/yr/yeenergiatasku2001.pdf 2001.

[3] Alakangas E. Properties of fuels used in Finland. Technical Research Centre of Finland, Research Notes 2045, Finland; 2000 [in Finnish].

[4] Huhtinen M, Hotta A. Combustion of bark. In: Gullichsen J, Fogelholm C-J, editors. Chemical pulping, vol. 6B. Helsinki, Finland: Papermaking Science and Technology; 1999. p. 205–305.

[5] Wimmerstedt R. Recent advances in biofuel drying. Chemical Engineering and Processing 1999;38:441–7.

[6] Fagernäs L, Sipilä K. Emissions from biomass drying. Proceedings of the Conference on Developments in Thermochemical Biomass Conversion, Banff, Canada; 20–24 May, 1996. 15p.

[7] Brennan D. Process industry economics. United Kingdom: Institution of Chemical Engineers; 1998.

[8] Pakowski Z, Mujumdar AS. Basic process calculations in drying. In: Mujumdar AS, editor. Handbook of industrial drying. New York, USA: Marcel Dekker; 1995. p. 71–112.

[9] Keey RB. Drying: principles and practice. New Zealand: Pergamon Press; 1972.

[10] Holmberg H, Ahtila P. Drying phenomena in a fixed bed under bio fuel multi stage drying. In: Oliveira A, Afonso C, Riffat S, editors. Proceedings of the First International Conference on Sustainable Energy Technologies. Porto, Portugal; 12–14 June, 2002. p. EES 6–11.

[11] Kunii D, Levenspiel O. Fluidization engineering. Stoneham, USA: Butterworth-Heinemann; 1991.

[12] Saastamoinen J, Impola R. Drying of biomass particles in fixed and moving beds. In: Strumillo C, Pakowski Z, Mujumdar AS, editors. Drying 96. Proceedings of the 10th International Drying Symposium (IDS 96). Krakow, Poland; 30 July–2 August, 1996. p. 349–56.

[13] Lampinen MJ. Chemical thermodynamics in energy engineering. Publications of laboratory of applied thermodynamics. Finland: Helsinki University of Technology; 1997 [in Finnish].